

Review and current status of SPECT scatter correction

This article has been downloaded from IOPscience. Please scroll down to see the full text article.

2011 Phys. Med. Biol. 56 R85

(<http://iopscience.iop.org/0031-9155/56/14/R01>)

View [the table of contents for this issue](#), or go to the [journal homepage](#) for more

Download details:

IP Address: 82.242.4.230

The article was downloaded on 04/07/2011 at 09:35

Please note that [terms and conditions apply](#).

TOPICAL REVIEW

Review and current status of SPECT scatter correction

Brian F Hutton¹, Irène Buvat² and Freek J Beekman^{3,4}

¹ Institute of Nuclear Medicine, UCL and UCLH NHS Foundation Trust, London, UK

² IMNC, UMR 8165 CNRS, Paris 7 and Paris 11 Universities, 15 rue Georges Clémenceau, 91406 Orsay Cedex, France

³ Section Radiation, Radionuclides & Medical Imaging, Delft University of Technology, Delft, The Netherlands

⁴ MILabs, Utrecht, The Netherlands

E-mail: brian.hutton@uclh.nhs.uk

Received 7 February 2011, in final form 27 April 2011

Published 23 June 2011

Online at stacks.iop.org/PMB/56/R85

Abstract

Detection of scattered gamma quanta degrades image contrast and quantitative accuracy of single-photon emission computed tomography (SPECT) imaging. This paper reviews methods to characterize and model scatter in SPECT and correct for its image degrading effects, both for clinical and small animal SPECT. Traditionally scatter correction methods were limited in accuracy, noise properties and/or generality and were not very widely applied. For small animal SPECT, these approximate methods of correction are often sufficient since the fraction of detected scattered photons is small. This contrasts with patient imaging where better accuracy can lead to significant improvement of image quality. As a result, over the last two decades, several new and improved scatter correction methods have been developed, although often at the cost of increased complexity and computation time. In concert with (i) the increasing number of energy windows on modern SPECT systems and (ii) excellent attenuation maps provided in SPECT/CT, some of these methods give new opportunities to remove degrading effects of scatter in both standard and complex situations and therefore are a gateway to highly quantitative single- and multi-tracer molecular imaging with improved noise properties. Widespread implementation of such scatter correction methods, however, still requires significant effort.

(Some figures in this article are in colour only in the electronic version)

1. Introduction

‘Scatter is the enemy’ is a quotation attributed to the late Ed Hoffman in the context of positron emission tomography (PET) but it is an equally valid statement in the context of single-photon

emission computed tomography (SPECT). In most clinical situations scattered photons account for 30–40% of the photons detected in the photo-peak energy window of a SPECT system. The presence of scatter results in a blurring and haziness of the observed projections, reduces reconstructed contrast and introduces significant uncertainty in quantification of the underlying activity distribution (Jaszczak *et al* 1981, Beck *et al* 1982, de Vries *et al* 1999). When applying modern scatter correction methods, improved quantification, lesion detection and contrast-to-noise ratios are achievable (e.g., Beekman *et al* 1997b, Buvat *et al* 1998, Frey *et al* 2002, Xiao *et al* 2006, 2007) although demonstration of benefit in clinical trials is lacking.

There have been many papers on scatter correction techniques published in the past 30 years including several reviews (Buvat *et al* 1994, Rosenthal *et al* 1995, Zaidi and Koral 2004a, 2004b, Zaidi 1996) and comparative studies (e.g. Gilardi *et al* 1988, Ljungberg *et al* 1994, Buvat *et al* 1995b, Beekman *et al* 1997b). In the review article published by Buvat *et al* (1994), the authors concluded that in practice only very basic methods for correction were routinely used. Fifteen years later this situation has not dramatically changed with many laboratories at best only implementing simple dual or triple energy window (TEW) subtraction techniques. The opinion of many practitioners is that simple scatter correction algorithms provide sufficient correction given that the influence of scatter on image quality is secondary to other factors such as attenuation and motion. In the meanwhile, development of scatter correction methods has continued to grow, particularly the development of model-based approaches including those that incorporate detailed Monte Carlo scatter estimation. However, there has been limited widespread acceptance of these correction methods and lack of concerted efforts to confirm robust application of these methods across institutions. The routine implementation by commercial suppliers has lagged seriously behind development. Few methods have undergone multi-centre validation and most site-specific developments have failed to attract wider implementation due to a variety of reasons.

In this review, we revisit the subject of scatter and its correction and have elected (i) to focus particularly on a range of the approaches that offer potential for routine implementation, and highlight what may be needed for these methods to become reality and (ii) to focus on recent approaches that offer quantitative scatter correction together with improved signal-to-noise ratio for a wide range of radionuclides and combinations thereof. These latter methods are enabled by the rapid increase of computer power, faster statistical image reconstruction methods, new methods of calculating scatter responses on-the-fly, more comprehensive SPECT data (e.g. more energy windows or even list mode data) and high quality attenuation maps provided by SPECT/CT. In addition we briefly address specific scatter correction issues in the rapidly growing field of small animal SPECT. Finally we discuss possible future directions including those in which scatter might be considered a friend, rather than a foe!

2. Understanding scatter

2.1. Compton and coherent scatter

The interaction of gamma photons with matter is well understood, the primary effects being photoelectric conversion (in materials of high atomic number) and either Compton or Rayleigh (coherent) scattering, which involve deflection of the photon with and without energy loss, respectively (figure 1). While the photoelectric effect is the main mechanism of interaction of photons in detectors, it is normally assumed that Compton scattering is the primary effect in tissue. Coherent scattering is predominant compared to Compton scattering below 150 keV; however, the deflection angle is small and coherent scattered photons are therefore not distinguished from primary photons. Most approaches to scatter correction therefore are

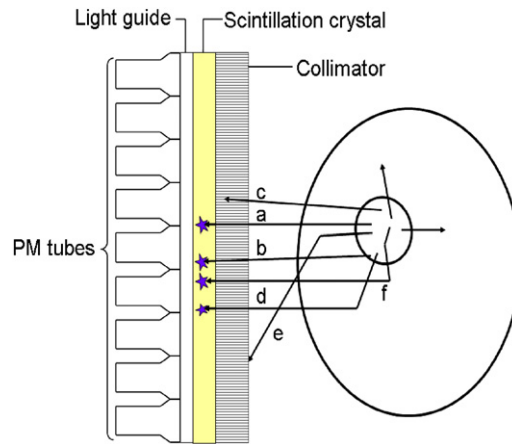


Figure 1. Cross-section through a patient with emitting organ and scintillation gamma camera with parallel hole collimator. Emitted gamma quanta with different trajectories are shown. (a) Ray that goes directly through the collimator parallel with a hole. (b) Ray that penetrates the collimator septum and is still detected. (c) Ray that is captured in the collimator because the angle deviates too much from hole direction and thus not detected. (d) Ray that results in scintillation after a single scatter event in the patient. (e) Ray that scatters in the patient, resulting in loss of photon flux (attenuation) but not in detected scatter. (f) Photon undergoing multiple scatter before generating a scintillation in the camera crystal.

based on consideration of Compton scatter only. When undergoing Compton scatter, photons lose energy depending on angle of deflection (θ) according to the formula

$$E_s = \frac{E}{1 + \frac{E}{m_0 c^2} (1 - \cos \theta)}, \quad (1)$$

where E_s and E are the energies of the scattered and incident photons, respectively, θ is the angle of scatter, m_0 is electron mass and c is the speed of light. It is normal practice to select an energy window within which photo-peak counts are acquired; choice of this energy window aims to maximize the number of primary non-scattered photons (given that these are detected over a range of energies defined by the energy resolution of the detector), while minimizing the number of scattered photons.

Since even relatively large angular deflections result in small loss of energy (from equation (1)), the detected scatter in the photo-peak energy window includes photons that have undergone significant angular deflection (figure 2(a)). With energy resolution of approximately 10% for a sodium iodide detector, there is still possibility that photons deflected through up to 90° can be detected within a 20% energy window. The distribution of scatter detected within the photo-peak energy window for a point source (point spread function: PSF) at depth in a uniform medium (e.g. water) is sometimes approximated by a mono-exponential function, although Monte Carlo simulation demonstrates that the distribution is better approximated by the sum of exponential and Gaussian functions (Narita *et al* 1996). Alternatively, mathematical analysis has shown that a K_0 Bessel function of the second kind convolved with a Gaussian function to model the collimator is a better description for the PSF than an exponential (Beekman *et al* 1993). Both number of scattered photons and their distribution are depth dependent. This is further complicated in practice where there are typically non-homogeneous tissues distributed within the body boundary; in general the scatter distribution is position and object dependent. Correction strategies therefore need to account for the number of scattered photons (often

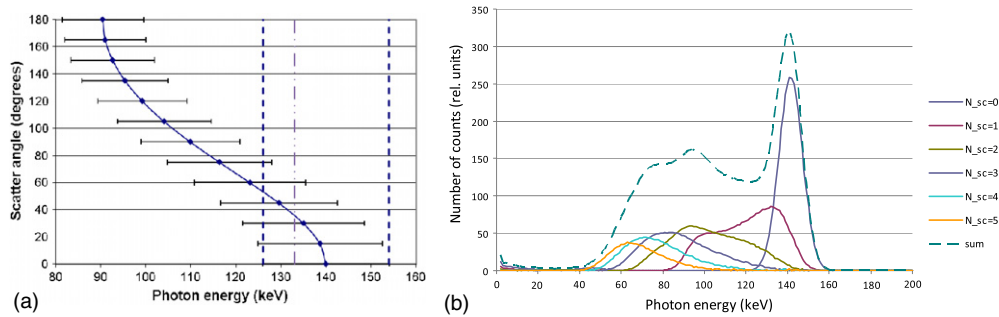


Figure 2. (a) Resultant energy of a 140 keV photon after scattering through a given angle; the error bars reflect the range of detected energies due to energy resolution (assumed 10%). The range of scatter angles detected in a given energy window can be appreciated (20% symmetric and 15% asymmetric photo-peak energy windows are illustrated by vertical lines). (b) Energy spectra for photons that have undergone either no Compton interaction ($N = 0$) or various orders of Compton scatter ($N = 1$ –5). Also illustrated is the sum of these spectra. Data produced using SIMIND (Ljungberg and Strand 1989) for clinically realistic activity distribution in the NCAT phantom (Segars *et al* 1999) and a gamma camera with a 10% energy resolution (courtesy K Erlandsson, UCL).

defined by scatter fraction SF where $SF = \text{scattered}/\text{total counts in the photo-peak window}$) as well as the distribution of scatter ($s(r, \theta)$ where r is radial distance from the projected photon origin), which is source and object dependent. Most of the correction approaches make some approximation regarding these parameters. Clearly photons can undergo multiple Compton interactions with resultant further loss of energy and further deflection. Most multiple-scattered photons have detected energies below the photo-peak window lower boundary, although in the case of ^{99m}Tc , multiple-scattered photons can still account for up to 20% of the total scatter counts (figure 2(b)).

2.2. Detector effects

As mentioned in the introduction, the primary photon interaction with a scintillation detector is via the photoelectric effect, although photon scatter in the detector is possible and accounts for some uncertainty in event location. The scatter correction techniques tend to focus on scatter occurring outside the detector. There are, however, factors other than scatter that give rise to observed counts outside the photo-peak. It is important to recognize these potential sources of low energy photons so that they can be distinguished from scatter. Incomplete attenuation of photons in the detector can occur if the detector is not sufficiently thick; as a result, there can be non-scattered photons with a range of detected energies. For ^{99m}Tc and the typical 9.5 mm NaI(Tl) detector, this contribution is small, but for other higher energy radionuclides the effect can be significant. It is worth also mentioning that similar and more significant effects are visible in the spectra for solid-state detectors; in this case the photon interactions produce direct ionization, with charge collection resulting in a measurable electronic signal without need for light conversion. Solid-state detectors are pixelated and there are limitations in the charge collection that results in signal sharing between neighbouring pixels. As a result, the energy spectrum can have low energy counts deriving from non-scattered photons. Measurement in energy windows below the photo-peak cannot therefore guarantee to be free from non-scattered data. A further source of low energy spectral contamination is the interaction of photons with the collimator; for high Z materials (lead or tungsten), K x-rays may be produced

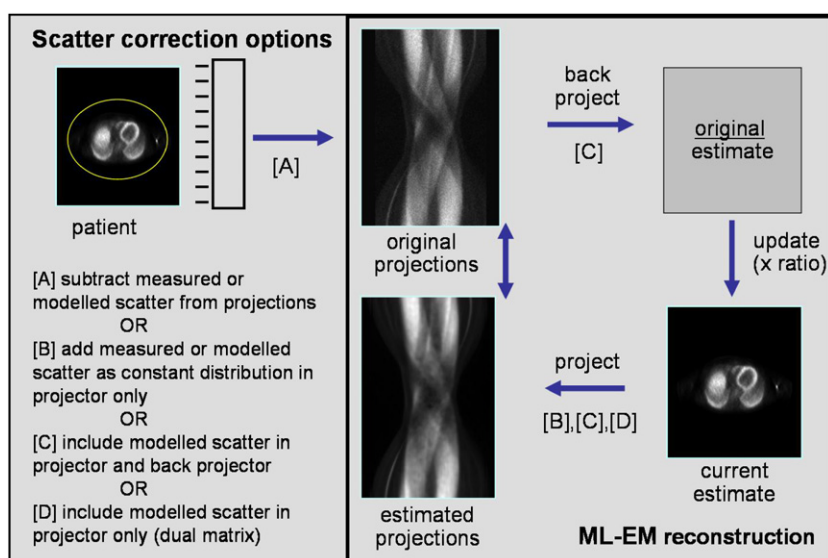


Figure 3. Options for scatter correction. Either subtract measured or modelled scatter directly from projections prior to reconstruction [A], or add measured or modelled scatter as a constant distribution in the projection step of the reconstruction [B] or directly incorporate a scatter model in both the forward- and backprojection steps of the reconstruction [C] or include the modelled scatter only in the forward projection step (using the dual matrix approach) [D].

with characteristic energies that may coincide with scattered photons. For example, lead K x-rays have characteristic energy of around 70 keV for photons emitted at 140 keV, coinciding with the main x-ray emissions from ^{201}Tl .

2.3. Basis of scatter correction approaches

There are many proposed approaches for the correction of scatter, perhaps contributing to the confusion as to what should be used clinically. The approaches range from those which are very simple and approximate, to others that attempt to achieve theoretically ideal correction but are so complex as to be, until recently, computationally untenable. In general, scatter correction involves either direct measurement or modelling (or some combination) in order to estimate the scatter present in the acquired photo-peak image. It is important to distinguish two alternatives: correction based on a measured or modelled scatter estimate that is considered constant as opposed to a scatter estimate that is iteratively updated during reconstruction. In the former case, correction involves either direct subtraction of the scatter estimate from the acquired projections or incorporation into the iterative reconstruction, irrespective of whether measurement or modelling is used to estimate the scatter. In the latter case, the scatter estimate is normally included only in the forward projection step of the iterative reconstruction, although alternatively the scatter model can be incorporated directly in both the forward and backprojection steps of the reconstruction (figure 3). Inclusion in the forward projection only (dual-matrix reconstruction) results in approximately the same favourable signal-to-noise properties as including scatter also in the backprojections (Kamphuis *et al* 1998) but has tremendous advantages in reducing computation time and required computer memory when scatter can be simulated quickly ‘on-the-fly’ (e.g. Beekman *et al* 2002).

In section 3, we first discuss approaches that are commonly used to compensate for scatter rather than employing actual correction strategies. The scatter correction approaches are broadly subdivided into those involving use of direct measurement (section 4), usually in several energy windows, as opposed to those that effectively model the scatter spatial response (section 5), although there is not always clear distinction in these methods; e.g. models are used in conjunction with multi-window spectral measurements. Section 6 is allocated to discussing a separate class of corrections designed for simultaneous measurement of multiple radionuclides and section 7 contains brief coverage of scatter correction in the context of preclinical imaging. Sections 8 and 9 include discussion on several alternative potential uses of scatter information and some practical issues.

3. Compensation without correction

3.1. Minimizing the amount of scatter

A technique which is commonly used in practice is to select an asymmetric photo-peak energy window so as to minimize the amount of scatter that is recorded. The technique does not eliminate scatter but can reduce the scatter fraction at the cost of also eliminating a fraction of the primary photons. A complication of using the technique is the uncertainty as to how much scatter has been removed, so choice of an effective attenuation coefficient is not straightforward and needs to be user-defined. The technique can lead to improved visual contrast in clinical images but is not ideal if quantification is required. A drawback of the approach is that uniformity correction usually is highly dependent on the selected energy window so uniformity correction tables need to be available for any specified asymmetric window (Buvat *et al* 1995a).

3.2. Modified attenuation correction

Scatter cannot be discussed without also referring to attenuation, which is the loss of primary photons compared to those detected in air. As photons travel through an attenuating medium, some undergo Compton scatter so that they no longer are detected; as a result the number of detected photons decreases exponentially with depth, dependent on the attenuation coefficient for the medium concerned. It should be noted that the probability of Compton interaction also depends on the attenuation coefficient at the point of interaction; it is therefore logical that measured transmission data can aid in modelling scatter as will be seen in later sections. It is usual to treat attenuation and scatter independently even though both result from the same Compton interactions; attenuation is considered the loss of primary photons that would have been detected in air; scatter is the addition of photons that would not have been detected in air, but are now detected at a displaced location. Attenuation correction strategies include simple multiplicative correction based on knowledge of the attenuation coefficients and hence the average attenuation factor for photons originating from a given location (Chang 1978). This approach is a reasonable first approximation for extremely focused activity distributions (close to a point source) and homogeneous attenuation. However, more accurate attenuation correction can now be performed by incorporating measured attenuation coefficients to determine the probability of detection during iterative reconstruction. Failure to correct for scatter prior to attenuation correction will lead to over-correction if standard 'narrow-beam' attenuation coefficients are used. These are attenuation values determined in the ideal situation where no scatter is present. In practice, scatter counts contribute to the total measured counts and hence there is less loss of photons than predicted from the idealized

'narrow-beam' values. This can be partly rectified by using instead 'broad-beam' attenuation coefficients, sometimes referred to as 'effective' attenuation coefficients that are smaller than the narrow-beam values, with values dependent on the photo-peak energy window width and centre-line as well as object size (Zaidi and Montandon 2002). For instance, at 140 keV, the narrow-beam attenuation coefficient is 0.15 cm^{-1} for water (or soft tissues), while the broad-beam value of 0.12 cm^{-1} (Harris *et al* 1984) is commonly used in practice. Often, a value is chosen that results in a uniform reconstructed activity for a uniform activity distribution rather than necessarily accurate activity concentration in the corrected reconstruction (use of first order Chang correction, even in the absence of scatter, tends to over-correct and so it is difficult to simultaneously achieve both accuracy and uniformity). However, this approach does not compensate for the spatial distribution of the object-dependent effects of scatter. Nevertheless, use of effective attenuation coefficients in conjunction with Chang attenuation correction continues to be a commonly used approach in clinical practice to roughly correct for the apparent reduction in reconstructed activity from deep structures, even though, generally, choice of appropriate parameters is poorly understood. This approach therefore compensates for the effect of scatter through a biased attenuation correction but cannot be considered a scatter correction technique as it does not remove photons that are at a wrong location. It is worth noting that similar care is necessary if utilizing a measured map of attenuation coefficients based on CT measurement, without performing scatter correction. Normally narrow-beam attenuation coefficients are derived using a bilinear equation to transform the measured Hounsfield numbers. In the presence of scatter, simply rescaling the resulting narrow-beam values provides an approximate solution, but since the scatter fraction is tissue-dependent, this scaling will not be exact. Ideally, both attenuation and scatter corrections should be performed, and whenever scatter correction is performed, attenuation should be compensated for using the narrow-beam, rather than broad-beam, attenuation coefficients.

3.3. Filtering

Historically, filtering was used to provide some compensation for scatter using filters such as Metz and Wiener filters which are designed to provide some degree of resolution compensation (e.g. King *et al* 1991). If the filter is derived from a PSF that includes scatter, then some contrast improvement is achieved. The problem with these filters is their assumption of a constant object-independent PSF, which is not true even without consideration of scatter. As a result these are no longer commonly used.

4. Scatter correction based on measurements

4.1. Dual and triple energy window corrections

One of the earliest scatter correction methods that was introduced for SPECT imaging involved the use of a lower energy window to measure a scatter image (Jaszczak *et al* 1984). The underlying premise was that the scatter image, scaled by an appropriate factor, k , provided an estimate of the scatter contribution that degrades the photo-peak window image. The main problem is that the spatial distribution of scatter differs as a function of both the loss of energy (equation (1)) and the different order of scatter; the primary window contains largely photons with small deflection angle, θ , and first order scatter, whereas a wide lower energy window will measure largely photons with large deflection angle and higher order scatter. The correction thus improves contrast by removing too many photons far from the actual source location and not enough at the source location. The method can also cause problems due to limitations in

uniformity correction that is highly energy window dependent (Buvat *et al* 1995a). The more recent TEW approach (Ogawa *et al* 1991) is similar in many respects; however, it relies on relatively narrow energy windows placed close on either side of the photo-peak. The scatter estimate SE is obtained on a pixel-by-pixel basis using

$$SE = \left(\frac{C_l}{w_l} + \frac{C_u}{w_u} \right) \times w_p/2, \quad (2)$$

where C_l and C_u are pixel counts measured in the lower and upper energy windows and w_l , w_u and w_p are the window widths for the lower, upper and photo-peak energy windows, respectively. The approach is general in the sense that it is intended to suit situations where there is down-scatter from higher energy emissions as well as scatter from the identified photo-peak emission; in the case of a radionuclide with only a single gamma emission the upper window can be assumed to have zero counts and can be eliminated (i.e. resulting in a dual energy window correction). The selection of scatter windows close to the photo-peak aims to achieve good estimation of the scatter distribution while also providing a realistic estimate of the scatter fraction. The approach involves subtraction of the scatter estimate pixel by pixel from the photo-peak projection image.

The TEW method has often been adopted as the standard approach to scatter correction, largely due to its simplicity and effectiveness in quite complex scatter situations. A definite advantage over the original dual energy method is that there is no need to calibrate the k weighting factor, as it is automatically derived from the width of the narrow and photo-peak energy windows (equation (2)). This makes it relatively easy to apply for any radionuclide and energy windows. A multi-centre trial has been conducted in Japan, possibly the first to include standardized scatter correction (Shinohara *et al* 2000). The major advantage is that the measurement reflects scatter independent of the distribution of activity (including out-of-field activity which is very hard to model). The main disadvantage (also compared to the dual window method that historically used a broader scatter window) is the noise amplification that arises due to acquiring relatively low counts in the necessarily narrow scatter windows, accentuated by pixel-by-pixel subtraction. This can be reduced by filtering the projection data acquired in the main and narrow scatter windows (Ichihara *et al* 1993, Hashimoto *et al* 1997). Selecting wider scatter windows can also reduce noise but, as pointed out above, the estimated distribution of scatter will likely be more biased. In low-count situations the presence of negative values in scatter-corrected projections can lead to serious artefacts. King *et al* (1997) found in a simulation study that normalized mean square error (NMSE) between phantom and images could be reduced by adding the scatter measurement to the forward projection estimate during iterative reconstruction instead of subtracting the scatter prior to reconstruction (refer to figure 3). This is illustrated in equation (3) which is the formula for maximum likelihood reconstruction according to Lange and Carson (1984) in which the additional scatter term (S_j) is included:

$$a_i^{n+1} = \frac{a_i^n}{\sum_j \tilde{M}_{ji}} \sum_j \frac{\tilde{M}_{ji} p_j}{\sum_i \tilde{M}_{ji} a_i^n + k \cdot S_j}, \quad (3)$$

where a_i^n is the activity estimate in voxel i at iteration n , p_j is the amount of counts detected within the photo-peak of pixel j , \tilde{M}_{ji} is matrix element representing the probability that a *primary* photon emitted from a voxel i will be detected in pixel j , k is a scaling factor that, in case of the definition in equation (2), will normally be set to 1. A similar approach was previously suggested for handling both scatter and random coincidences in PET reconstruction (Bowsher and Floyd 1991). Adding the scatter in the denominator of the ML-EM or OS-EM algorithm has two benefits. Firstly this avoids the subtraction

process that negates the assumption of Poisson distributed projection counts, an assumption that is inherent in maximum likelihood algorithms. In addition, direct subtraction can result in negative projection counts that cannot be accommodated in conventional maximum likelihood reconstruction leading to bias and possible artefacts (Beekman *et al* 1997b, Hutton and Baccarne 1998). Note that, as outlined in section 2.3, equation (3) can be generally applied to incorporate any scatter estimate based on measurement or model. Alternatively S_j can be updated based on improved estimates of the activity distribution during the iterative reconstruction.

4.2. Other energy window approaches

Several groups have developed approaches based on measurements in two or more energy windows. These include the dual photo-peak window method using two windows to split the photo-peak (King *et al* 1992, Pretorius *et al* 1993) and multi-energy window approaches that estimate the scatter image detected in the photo-peak energy window as a linear combination of images detected in multiple energy windows (e.g. Vija *et al* 1999) (see also later sections). None of these techniques managed to over-ride the simpler dual or TEW approaches for practical reasons. Indeed, all involved more than two parameters to be tuned (similar to weights to be associated with each energy window) with no easy practical recipe to determine these weights for a specific imaging protocol. In addition, as previously explained, using a broad range of energy windows requires uniformity corrections appropriate for each energy window, which are not necessarily provided on the gamma cameras (Buvat *et al* 1995a). Given that the performance of all these approaches are rather similar, without any clear advantage in using the more sophisticated ones (Ljungberg *et al* 1994, Buvat *et al* 1995b, Assié *et al* 2010), only the simplest dual and triple energy approaches have withstood the test of time.

4.3. Spectral models

Considerable effort was expended in the 1990s on developing various approaches to scatter correction that were based on more extensive spectral analysis and modelling. These rely on recording precise energy information for all detected events, and fitting the energy spectrum of events detected in each pixel using a model from which the scatter and primary contributions could be distinguished. These methods included spectral fitting (Koral *et al* 1988), factor analysis (Mas *et al* 1990, Buvat *et al* 1993, Hapdey *et al* 2006) and holospectral imaging (Gagnon *et al* 1990). Despite the rather high accuracy of these corrections (Buvat *et al* 1995b), with the added advantage of being non-stationary and appropriate to compensate for scatter coming from out-of-field activity, their implementation required either full list-mode acquisition including energy information or simultaneous acquisition of data in a large number (> 10) of energy windows, neither being commonly available at that time. This prevented them from undergoing thorough evaluation and comparison with simpler methods on clinical data, steps that are usually required for sophisticated methods to become widely accepted.

There is currently a tendency for list-mode acquisition to be more widely used by suppliers as part of their processing chain in recent instrument designs and this facility is sometimes available to research groups. Developments in this area therefore might resurrect interest in this category of approaches, provided it can be first shown that performance is significantly better than that of simpler methods or the recent generation of very fast fully 3D Monte Carlo based correction methods. Although this is uncertain for ^{99m}Tc or even ^{123}I scans, the methods based on spectral models might warrant further consideration for radionuclides with more complex decay schemes like ^{201}Tl , ^{67}Ga or ^{131}I and in dual radionuclide acquisitions (see section 6).

4.4. 'Failed' commercial approaches

A number of approaches to scatter correction have been incorporated in commercial systems, particularly hardware-based approaches. However it is notable that these approaches have not been continued in more recent systems. Examples are the 'Compton Free Imaging (CFI) introduced by Elscint and the 'Weighted Acquisition Module' (WAM) introduced by Siemens.

CFI (Maor *et al* 1991) was similar to the spectral fit mentioned in section 4.3: acquisitions were performed in a large number of narrow energy windows (typically 16 windows of 3.5 keV from 105 to 161 keV for $^{99\text{m}}\text{Tc}$), so that a finely sampled energy spectrum was available for each pixel of the acquired projections. These observed spectra were then fitted independently (1 fit for each pixel) using a least-squares procedure onto a set of reference spectra consisting of one primary spectrum (corresponding to unscattered photons) and a number of scatter spectra (one for each scatter order to be included in the model). The reference scatter spectra were derived from the Klein–Nishina equations, accounting for the energy resolution of the gamma camera. The approach was demonstrated to be effective in breast studies (Nunez *et al* 2002), but had some practical limitations. Although it has the advantage of being non-stationary, the main limit was the instability of the large system of equations due to the high noise affecting the finely sampled spectra corresponding to individual pixels (Monville and O'Connor 1997).

In the WAM module implemented by Siemens (Halama *et al* 1988, DeVito *et al* 1989), each detected event was redistributed in a 21 pixel region centred on the detection pixel. The redistribution map depended only on the energy of the detected event (not on the position) and included positive and negative weights (DeVito and Hamill 1991). The redistribution maps were stored in the system (no parameter to adjust for the user) and the corrected image was produced in real time and displayed next to the uncorrected image. This method underwent some clinical evaluation with encouraging results (Hamill and DeVito 1989, Floyd *et al* 1991). However, the method had two important limitations: first, it assumed a stationary scatter response function, which is known to be incorrect, and second, the spatial weighting introduced some correlated noise in the projections, which propagated through the reconstruction (Jaszczak *et al* 1991). These limitations, as well as the fact that the pre-determination of robust weighting maps was challenging, probably explain why the WAM module has been abandoned.

5. Scatter correction based on modelling the scatter distribution

5.1. Motivation for modelling approaches

During the eighties and nineties, iterative methods like ML-EM (Shepp and Vardi 1982, Lange and Carson 1984) and accelerated versions thereof became more and more popular. The theoretical advantage of these algorithms with regard to noise properties, convergence, etc, over other iterative methods or direct methods of reconstruction such as filtered backprojection (FBP) is achievable only if the detection probabilities M_{ji} can be well modelled. Of course this is only possible if an accurate model of scatter is available, which needs to be sufficiently practical to be incorporated in the transition matrix, calculated on-the-fly or modelled as a background term (equation (3)). The first attempt in SPECT to create such a matrix including all image degrading effects was carried out at Duke university (Floyd *et al* 1986). However, due to (i) limited computer memory and speed and (ii) lack of acceleration methods for both Monte Carlo simulation and iterative statistical reconstruction available at that time, this method needed to be restricted to 2D implementation, which ignored photons scattering outside each transaxial plane or used a simplified way to estimate these scatter components

(Bowsher and Floyd 1991). Despite these limitations, the concepts introduced in these publications were extremely inspiring for many research groups who in the years thereafter attempted to find methods to incorporate accurate models of the full 3D scatter response in the transition matrix, often referred to as reconstruction-based scatter correction.

An important question was of course if such a tedious scatter modelling would have clear advantages over other methods. As discussed, scatter subtraction before MLEM or adding scatter in the denominator of an MLEM method has the disadvantage that noise properties of the reconstructed image are not optimal: one adds little information from scatter window data and these data are noisy. Extensive simulation studies (Beekman *et al* 1997b, Kadrmas *et al* 1998) were performed in which it was shown that accurate modelling of the full 3D spatial scatter response is superior in terms of noise properties (contrast-to-noise ratio as a function of iteration number) compared to using window-based scatter correction, even if the window-based scatter estimate is noise-free (which is better than can be achieved in practice). Several other simulation studies confirmed the superiority of modelling approaches (Frey *et al* 2002, Gur *et al* 2002, Narayanan *et al* 2003, Lazaro *et al* 2005, Xiao *et al* 2006). In the following sections a range of approaches to modelling scatter are discussed as well as the different strategies that have been developed to efficiently incorporate scatter during reconstruction. A limitation of these approaches, however, is that, unlike the methods based on the use of several energy windows, they do not account for scatter coming from activity present outside the field-of-view. Methods to address this problem have been suggested for cardiac perfusion imaging (Xiao *et al* 2000) although these have not as yet been demonstrated to be generally applicable to other studies.

5.2. Analytical models based on Klein–Nishina scatter equations

A number of authors have published descriptions of the analytical equations that allow an exact calculation of scatter. These are quite complex, incorporating transport of photons from source to detector with probability of Compton interaction at any point (e.g. Riauka and Gortel 1994, Riauka *et al* 1996, Wells *et al* 1998). Estimation of scatter using these models is extremely demanding computationally, because it involves calculation of high dimensional integrals. Analytical methods are thus usually restricted to modelling first order scatter, although in theory these could be expanded to accommodate multiple order scatter.

A useful simplification to these approaches has been proposed by Welch *et al* (1995) who approximated the probability of photons being scattered at a specific location so as to be detected in the photo-peak energy window by the product of a Gaussian (as a function of deflection angle) and the local attenuation coefficient; parameters were determined by fitting Monte Carlo data. The technique was later validated for 3-dimensional implementation (Laurette *et al* 2000) but was still very slow. Instead of having statistical noise that potentially hampers Monte Carlo methods, for practical implementation these models need a sparse sampling of the function during integration, resulting in inaccuracies and discretization errors (e.g. Kadrmas *et al* 1998).

5.3. Transmission-dependent convolution subtraction

A simplified model for scatter based on the (mis) assumption that the scatter point response could be accurately modelled as a stationary mono-exponential function was introduced at an early stage (Axelsson *et al* 1984, Msaki *et al* 1987). The approach estimated scatter based on a convolution of the photo-peak counts by this function with parameters optimized by experiment or Monte Carlo simulation (assuming that the photo-peak counts, to a first

approximation, represent the scatter-free projection); estimated scatter was then subtracted from the photo-peak counts or incorporated in the reconstruction modelling. As was later shown, this is best applied to the geometric mean of opposing projections so as to minimize depth-dependence and the technique can be applied iteratively (Bailey *et al* 1989) reaching a satisfactory solution in a small number of iterations. The same group also introduced the use of a correction factor based on transmission measurement that markedly improved the scatter estimation, effectively compensating for the assumption of a stationary scatter distribution. This method, extended by Meikle *et al* (1994), is referred to as transmission-dependent convolution subtraction (TDCS) and has been extensively studied. It was demonstrated to be superior to TEW using Monte Carlo simulation (Narita *et al* 1996) and the optimal model parameters (using a combined mono-exponential and Gaussian) were demonstrated to be independent of collimator (Kim *et al* 2001a) and applied with good results in studies of brain (Iida *et al* 1998, Kado *et al* 2001, Shidahara *et al* 2002) and heart (Eberl 2000, Iida *et al* 2008). The technique is approximate and bears some resemblance to the slab-based corrections described below. The appeal is in the relatively simple implementation compared to more complex models. The technique does require measured transmission data, less of a problem with the increased availability of dual modality systems. The method also relies on having geometric mean of opposing projections, which requires a modification of standard reconstruction algorithms, although a similar approach has been described for 180° acquisition (Hutton *et al* 1996) and the more general case without need for geometric mean data (Hutton and Baccarne 1998). The approach more recently has been further developed for application in object space rather than projection space (Shidahara *et al* 2005) and as a single step correction applied during reconstruction rather than a two-step process (Sohlberg *et al* 2008a).

5.4. Object shape or slab-derived scatter estimation

Other groups have developed alternatives to MC or Compton equation-based scatter models, mainly motivated by the need to have computationally efficient estimation that incorporates a non-stationary scatter distribution in MLEM-type algorithms (Beekman *et al* 1993, 1997a, Beekman and Viergever 1995, Frey *et al* 1993, Frey and Tsui 1993, 1996, Kadrmas *et al* 1998, Kamphuis *et al* 1998). Their approaches rely on experimental or Monte Carlo simulation to tabulate scatter functions at various depths behind a slab of water. These functions can be very accurately extended to uniform objects of various shapes (Beekman *et al* 1993, 1994, Frey *et al* 1993). Transport through non-homogeneous tissues is then approximated by establishing slabs representing water-equivalent depths through which photons are tracked (e.g. Beekman and Viergever 1995, Frey and Tsui 1993). Frey extended on this work with development of effective scatter source estimation (ESSE) where the attenuation from each point of Compton interaction to the detector is incorporated in the model. Similar assumptions are used to those in TDCS since the model effectively ignores the attenuation between source and point of Compton interaction, treating this effect as a secondary effect that is approximated by the scatter kernel (which assumes homogeneous attenuation). ESSE has been demonstrated to provide good results in a range of applications (Du *et al* 2006, Farncombe *et al* 2004). Another alternative to handle non-uniformities in slab-based scatter response approaches was developed in Beekman *et al* (1997a).

5.5. Reconstruction-based scatter correction: general

As mentioned earlier, pre-calculated or measured scatter can be incorporated by simple addition of this constant estimate in the denominator of the ML-EM or OS-EM equation during

reconstruction. The alternative is to directly include a scatter model in the system matrix which defines the probability of photons emitted from each object voxel being detected in a specific detector pixel (Floyd *et al* 1986, 1989, Bowsher and Floyd 1991, Laurette *et al* 2000, Lazaro *et al* 2005). The final solution then includes information from the scatter photons as part of the overall solution, with potential benefits in terms of signal-to-noise. The downside is that the system matrix becomes very large and as a result convergence requires relatively high number of iterations and computation speed is slow. The model used for scatter estimation can be pre-calculated but is object-dependent, based on the distribution of tissue densities. It is therefore unique to each patient.

If efficient and accurate models of scatter can be incorporated directly in reconstruction, there is scope to consider a wider range of energies in an attempt to utilize the additional photons to further improve signal-to-noise in the reconstruction. The inclusion of additional scatter degrades the acquired data, even if improving the overall statistics; the overall merit depends on whether there is net gain in including additional scatter photons in more complex system models. This possibility was explored fairly extensively (Beekman *et al* 1997b, Kadrmas *et al* 1998) with both groups concluding that there was potential merit in including measured scatter counts during reconstruction, but both also agree that this could not improve on perfect scatter rejection. Kadrmas *et al* (1998) additionally concludes that improvement could be achieved if it were possible to separately label scatter and primary counts in the photo-peak window, but this is clearly not feasible. He also suggests that there is limited scope to further improve reconstruction by including acquisition of multiple scatter windows.

5.6. Reconstruction-based scatter correction: incorporation of fast Monte Carlo scatter estimation

Rather than using some simplified form of model to estimate scatter, a full Monte Carlo (MC) simulation can be applied. Given knowledge of the distribution of attenuation coefficients the scatter distribution for individual sources of activity can be accurately estimated. MC has been used for some time to aid in defining scatter kernels for use in scatter correction (e.g. Ljungberg and Strand 1990, Koral 1998). Full estimation of scatter for an individual patient was traditionally considered too computationally demanding to be practical especially if the scatter has to be re-estimated after every iteration. Recent work in optimizing MC, however, has demonstrated that it is feasible to compute scatter estimates sufficiently fast to be practical to include it in statistical image reconstruction (Beekman *et al* 2002, Ouyang *et al* 2007, Sohlberg *et al* 2008b).

A computationally efficient fully 3D MC-based reconstruction architecture that compensated for non-uniform attenuation, full 3D scatter effects and distance-dependent collimator response was proposed in Beekman *et al* (2002). The method included (i) a dual matrix ordered subset reconstruction algorithm (Kamphuis *et al* 1998) to accelerate the reconstruction and completely avoid the need for massive transition matrix pre-calculation and storage (ii) a stochastic photon transport calculation combined with a straight forward analytic model of how photons are detected after a scatter event in the body. Convolution forced detection (CFD) as explained below (Beekman *et al* 1999, De Jong and Beekman 2001a, De Jong *et al* 2001b) was used to dramatically reduce noise in the Monte Carlo based re-projection after only a small number of photon histories had been tracked. In addition, an option was proposed in which the number of photon histories simulated was reduced by an order of magnitude in early iterations, or photon histories calculated in an early iteration were reused. The reconstruction time required for such MC-based methods today is often less than

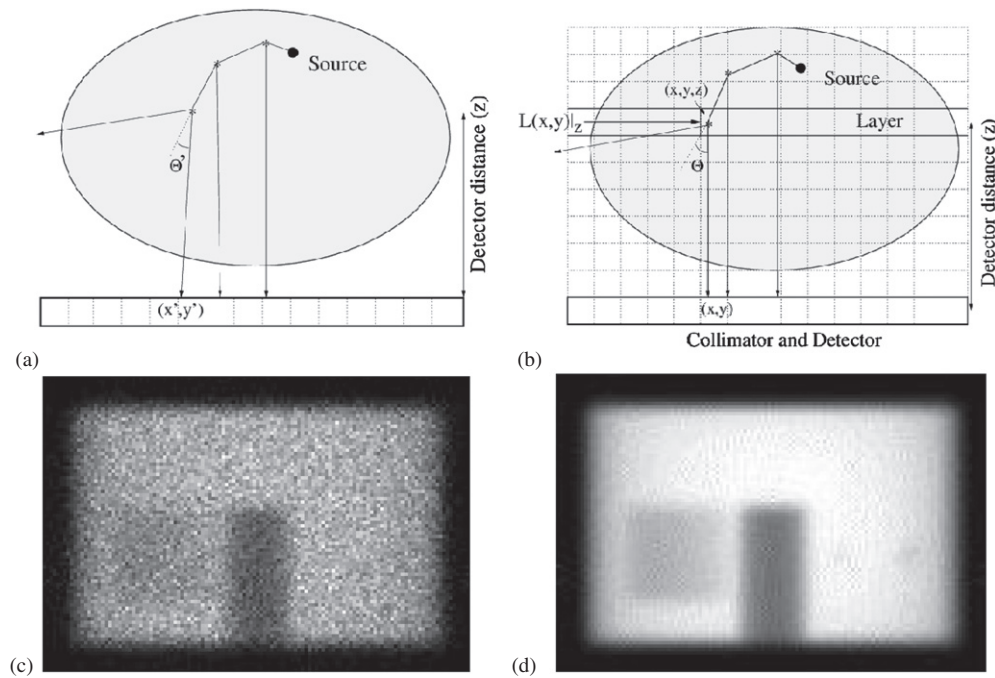


Figure 4. (a) Principle of standard forced detection (FD) where photons at each scatter point are forced stochastically to the detector. (b) Principle of convolution forced detection (CFD): photons are forced parallel to the collimator hole axis and only the photon weights of these photons are calculated and their sum is stored in voxels. Voxels in layers $L(x, y)$ at different distances z from the collimator are convolved with an appropriate distance-dependent collimator response that is pre-stored in a table. The noisy FD-based re-projection (c) and almost noise-free CFD-based re-projection (d) are based on the same number of photon histories (figure adapted from de Jong *et al* 2001b, Beekman *et al* 2002).

a minute on a standard PC, in which case the slightly stochastic nature of MC-CFD modelling has a negligible effect on noise in reconstructions (De Wit *et al* 2005).

Forced detection is a standard method to accelerate Monte Carlo simulation in which a photon that scatters is forced to travel towards the detector within the acceptance angle of the collimator (figure 4(a)). This latter step of choosing the photon angle is stochastic, so each scatter point in the object would produce a small noisy cloud on the simulated projection. CFD avoids this noise-generating last step by using tables of the distance-dependent collimator response to facilitate convolution for layers of voxels each containing accumulated photon weights that are generated with MC simulation (figure 4(b)) instead of modelling the detection process stochastically. Figures 4(c) and (d) show the difference in projection one gets by using FD or CFD, respectively, for the same number of object photon tracks. CFD and similar methods greatly reduce the required number of simulated photons to achieve effectively noise-free MC simulation (with computation time reduce typically by 50–100 compared to FD). It clearly outperforms alternative approximate scatter models (Beekman *et al* 2002) but does require optimized software that until recently has not been generally available.

CFD has been validated for ^{99m}Tc (de Jong *et al* 2001b, Liu *et al* 2008, De Beenhouwer *et al* 2008), although this did not include any septal penetration component. Fast methods were developed for incorporating these effects and were validated for ^{201}Tl and ^{111}In (Staelens *et al*

2007, Liu *et al* 2008). Also, instead of using traditional PSFs, angular response functions (ARFs) have been proposed (Song *et al* 2005), applying similar principles as CFD that include an accurate model of the photon interaction with the collimator. As in CFD, the use of ARFs removes the need for tracking the photons inside the collimator/detector volumes, which in turn yields significant reductions in run time.

Clinical evaluation of these techniques is currently hampered by the lack of general availability of executable code. CFD has been incorporated in available MC packages such as SIMIND (Khosravi *et al* 2007) and both CFD and ARF have also been recently incorporated in GATE (Descourt *et al* 2010). It should, however, be pointed out that the computation speed can remain slow, even if acceleration is achieved. Fast executable code for MC-based scatter correction specifically for incorporation in statistical reconstruction is now available from Nuclear Diagnostics (Sohlberg *et al* 2008b) or may be obtained for research purposes on request from University of Utrecht⁵ (Beekman *et al* 2002).

6. Incorporating multiple energy windows

6.1. Multi-radionuclide SPECT

Because of energy discrimination capabilities, SPECT systems can simultaneously acquire images of two or more tracers, each labelled with a radionuclide emitting photons of different energies. This simultaneous imaging capability has several potential advantages, including reduced patient discomfort and lower acquisition time, and even more important, production of images that are perfectly registered in space and time. In recent years, several dual probe imaging protocols (e.g., labelled with ^{99m}Tc and ¹²³I, or ²⁰¹Tl and ^{99m}Tc) have been developed for SPECT imaging. The main complication in multi-radionuclide imaging arises due to spill-over effects caused by down-scatter from higher energy emissions being detected in the lower energy photo-peak(s). The down-scatter, unlike scatter in the photo-peak, is a result of higher order scatter, which can be difficult to estimate. The model is more complex in the case of ²⁰¹Tl due to the presence of lead x-rays in the same energy range as the ²⁰¹Tl x-ray emissions. The model is further complicated in the case of solid-state detectors since there is also a low energy component due to incomplete charge detection in the detector that cannot be easily separated from lower energy peaks.

Multiple energy windows can be used, estimating scatter in each photo-peak energy window based on projections acquired in other energy windows, either using adaptations of the TEW approach (e.g. Matsudaira *et al* 1997) or using convolution models to derive the relationship between the primary and scatter projections recorded in different energy windows (Moore *et al* 1995, Knesaurek and Machac 2000). A set of simultaneous equations can be established to describe the various components in each of several energy windows and these can be used to derive scatter-free photo-peak projections using artificial neural networks (El Fakhri *et al* 2001), spectral factor analysis (Hapdey *et al* 2006) or maximum likelihood estimation (Kacperski *et al* 2011). In this latter case, the combination of better energy resolution (<6%) in combination with tungsten collimators also permitted separation of the tungsten K x-rays. This has been recently demonstrated in dual ²⁰¹Tl/^{99m}Tc cardiac studies (Ben-Haim *et al* 2010).

Considerable recent effort has been directed to implementing dual radionuclide correction via direct reconstruction with modelled crosstalk (de Jong *et al* 2002a, Du and Frey 2009, Du *et al* 2007, Ouyang *et al* 2007, 2009). The use of Monte Carlo in this work is particularly useful

⁵ Information about Utrecht Monte Carlo Software (UMCS) for research evaluation can be obtained from f.j.beekman@tudelft.nl.

as the overall model is quite complex and would be hard to emulate by simpler models. Again, use of MC is only possible given recent introduction of acceleration techniques that permit fast computation with suitably smooth estimates for multiple-order scatter. The effect of including detector and collimator effects simultaneous with down-scatter has been demonstrated (de Jong *et al* 2002b).

6.2. Multi-energy radionuclides

Similar considerations are relevant to the correction of scatter for radionuclides with multiple primary emissions of different energy (e.g. ^{123}I , ^{131}I , ^{111}In , ^{67}Ga) where scatter originating from higher energy photo-peak emissions contaminates measurements in lower photo-peak energy windows (Dewaraja *et al* 2000, Dobbeleir *et al* 1999). As in the case of dual radionuclide scatter correction strategies, the quantity and distribution of photons down-scattered into lower energy windows has to be estimated based on measurement or modelling. Unlike the dual radionuclide case where direct measurement can be used for validation purposes, the down-scatter and photo-peak scatter cannot be isolated. For practical purposes, methods based on the use of several energy windows have definite appeal (Assié *et al* 2010), despite their limitations, since they permit direct estimation of the combined scatter. Monte Carlo methods also have definite appeal in this context as the down-scatter and photo-peak scatter are independently modelled for direct inclusion in the reconstruction (Dewaraja *et al* 2006, Cot *et al* 2004, 2006). Corrections can also include the effects of septal penetration due to high-energy photons, which tends to be particularly problematic for some multi-energy radionuclides (El Fakhri *et al* 2002, He and Frey 2006). The combination of corrections has potential to significantly improve the diagnostic quality of multi-energy radionuclides which have traditionally been considered inferior.

7. Scatter correction in small animal SPECT

Imaging of small animals with SPECT is rapidly gaining popularity. Most of these devices are based on the use of pinholes that magnify projections of the radionuclide distribution on detectors that otherwise would not have been able to resolve the small details within such animals. Since the likelihood of undergoing scatter events in small animals such as mice and rats is much smaller than in human beings, the effects of photon scatter in tissue are smaller for the majority of these animals when the same radionuclides (with the same emission energies) are used as in clinical SPECT.

The relative amount of photons that have scattered in the pinhole is low even for tiny pinholes (van der Have and Beekman 2004, 2006). Because of the low amount of scatter only simple window-based corrections are often sufficient for $^{99\text{m}}\text{Tc}$, ^{123}I and ^{111}In (Hwang *et al* 2008, Vanhove *et al* 2009, Wu *et al* 2010). In the case of multi-peak spectra and multi-radionuclide imaging, however, it is important that several scatter windows are used. Some commercial small animal SPECT systems are suitably equipped with list mode data acquisition (e.g. van der Have *et al* 2009). When imaging radionuclides with additional high energetic contributions (i.e. ^{123}I) or contaminations such as present in ^{201}Tl (Staelens *et al* 2006, 2008) scatter in the collimator and detector can lead to a rather flat background that can easily be corrected by window-based methods.

There are situations where scatter problems in small animal SPECT differ from clinical SPECT: (i) scatter in the collimator, both in single and multi-radionuclide SPECT can be a significant problem, and (ii) in contrast with clinical systems, small animal SPECT systems often allow for imaging radionuclides with low energies like ^{125}I . Hwang *et al* (2008) found

that, when imaging ^{125}I , the scatter-to-primary ratio can reach up to approximately 30%, which can cause overestimation of the radioactivity concentration when reconstructing data with attenuation correction only.

Simulations in mouse-sized phantom studies showed that attenuation effects alone degraded quantitation accuracy by up to -18% ($^{99\text{m}}\text{Tc}$ or ^{111}In) or -41% (^{125}I) (Chen *et al* 2009). The inclusion of scatter effects changed the above numbers to -12% ($^{99\text{m}}\text{Tc}$ or ^{111}In) and -21% (^{125}I), respectively, indicating the significance of scatter in quantitative ^{125}I imaging, but also suggesting that scatter ‘is a friend’ when applying no correction for both attenuation and scatter. The authors also state that region-of-interest (ROI) definitions have greater impact on regional quantitative accuracy for small sphere sources as compared to attenuation and scatter effects. For the same ROI, SPECT acquisitions using pinhole apertures of different sizes could significantly affect the outcome (Chen *et al* 2009). This stresses the need for very high resolution in small animal SPECT.

Special attention to scatter correction may be needed for multi-radionuclide small animal SPECT. Although crosstalk may be less than in clinical SPECT, due to lower amounts of object scatter, scatter in the collimator and detector may be significant, for example in dual radionuclide SPECT using a combination of single-photon emitters and positron emitters (Goorden and Beekman 2010).

8. Potential uses of Compton scatter

8.1. Compton camera

The idea of Compton imaging was originally explored by Singh and Doria (1983). The technique is based on replacing the conventional collimator with a high energy resolution, solid-state detector, which detects the energy deposited during Compton scatter and so estimates the angle of deflection, from which the photon origin can be determined (figure 5). In practice, limited energy resolution imposes an uncertainty in the deflection angle and the photon origin can only be specified as lying within a thick conical surface. This information can be used to aid reconstruction but the gain in signal-to-noise is small, especially for low energy photons (An *et al* 2007, Harkness *et al* 2009a). Research is continuing in this field with current developments in low-noise, high spatial and energy resolution silicon (lithium doped) detectors providing significant efficiency gains, which offer potential for application at energies as low as 140 keV (Harkness *et al* 2009b). Also there is potential to isolate the direction of the recoil electron which would significantly improve the uncertainty in origin of the emission (Kurosawa *et al* 2010). These developments could in time mean that Compton cameras are serious contenders for clinical use.

8.2. Using scatter to determine attenuation maps

The possibility of performing attenuation correction without the need for transmission/CT data would have immediate clinical appeal. Several earlier papers suggest the use of scatter to highlight body boundaries or boundaries between lung and other soft tissue with the aim being to construct a segmented attenuation map for the purpose of attenuation correction (e.g. Zaidi and Hasegawa, 2003). This works well where activity is widely distributed as in lung SPECT studies (e.g. Pan *et al* 1997, Bailey *et al* 2008, Nunez *et al* 2009) and also has proved useful in brain SPECT studies (Barnden *et al* 2006). The technique does however have limitations when activity is focal.

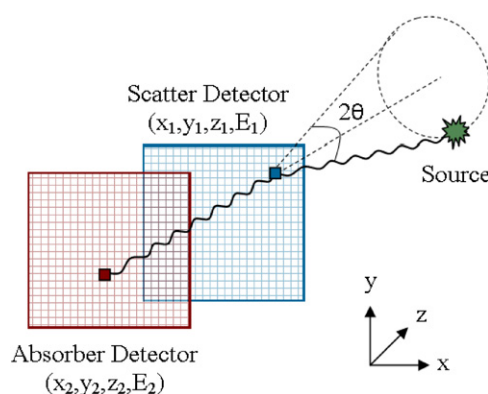


Figure 5. A schematic diagram of a dual layer Compton camera system showing the cone produced for one incident gamma ray which transfers energy E_1 to an electron via Compton scattering at position (x_1, y_1, z_1) in the scatter detector and then deposits its remaining energy E_2 through photoelectric absorption at position (x_2, y_2, z_2) in the absorber detector (courtesy Andrew Boston, University of Liverpool).

A number of researchers have previously attempted to derive an attenuation map directly from primary emission data, either using the differential attenuation for multi-energy emission (Vija *et al* 1999) or using consistency conditions for single-energy photon emission to extract an estimate of the attenuation (Bronnikov 2000, Nuyts *et al* 1999, Crepaldi and de Pierro 2007). The attempts to do this have met with limited success and have not been widely used. A promising alternative approach is to invert the models used to estimate scatter given that these are directly dependent on attenuation. Therefore given measured photo-peak and scattered projections the model can be used to determine the distribution of unknown attenuation coefficients so as to best match the measurements. Initial attempts to achieve this have demonstrated promising results (Cade *et al* 2010, Sitek *et al* 2007) suggesting that implementation may even be possible for 180° acquisition.

9. Practical considerations

9.1. Clinical impact of scatter correction

In the 1994 review on scatter correction (Buvat *et al* 1994), the lack of validation studies was highlighted. In recent years, there have been additional studies undertaken to demonstrate the usefulness of scatter correction for three specific purposes: to improve contrast and image quality, to improve quantification and to improve ability to acquire dual radionuclide studies. Unfortunately, there has been limited effort to standardize the approach to scatter correction in these studies and, as would be expected, comparison is usually made between data that are non-corrected as opposed to both attenuation and scatter corrected. Certainly it makes more sense to perform scatter correction in addition to attenuation correction particularly if there is non-homogeneous attenuation (Hutton 1997, El Fakhri *et al* 2000a). To the best of our knowledge, there has not been any patient-based observer study demonstrating that scatter correction improved lesion detectability, even if several studies based on phantom experiments demonstrated improved lesion detectability in scatter-corrected planar images (Buvat *et al* 1998) and increased contrast-to-noise ratios in SPECT scatter-corrected images (Xiao *et al* 2006, 2007). In general, authors have demonstrated that combined attenuation

and scatter correction has benefit in cardiac perfusion imaging (e.g. El Fakhri *et al* 2000a, Narayanan *et al* 2003, Xiao *et al* 2006, 2007); application of course depends on having availability of transmission data (nowadays implying dual-modality SPECT/CT imaging). The primary benefit in this application, however, is undoubtedly due to attenuation correction, unless absolute quantification is required (e.g. Iida *et al* 2008). There have been several demonstrations of benefit in brain studies where the contrast improvement can be significant (Iida *et al* 1998, Kado *et al* 2001, Shidahara *et al* 2002) mainly based on relatively simple approaches. There are a few papers that highlight advantage in other studies (He and Frey 2006, Farncombe *et al* 2004). What is worth emphasizing is the wide range of approaches adopted by different clinical researchers, contributing to the general confusion as to which method to adopt. For example in the quantification of the nigrostriatal dopaminergic system a wide range of scatter correction methods have been applied; this includes TDCS (Kim *et al* 2001b), artificial neural networks (El Fakhri *et al* 2000b), ESSE (Du *et al* 2006), TEW (Soret *et al* 2003), and Monte Carlo based correction (Cot *et al* 2005, Crespo *et al* 2008, Bullich *et al* 2010).

There is an increasing literature where absolute quantification is used either in the context of tracer kinetic analysis or dosimetry and scatter correction is demonstrated as essential in these studies. For example the conclusion drawn by Bullich *et al* (2010) is that scatter correction played a major role in accounting for the differences between ^{123}I -IBZM and ^{11}C -raclopride PET. In dosimetry studies, SPECT is playing an increasingly important role and scatter correction remains one of the essential components (Sgouros *et al* 2008, He and Frey 2006, Dewaraja *et al* 2005). Recent evaluation of the accuracy of quantitative SPECT suggest that activity concentration can be estimated to around 5% accuracy in phantoms (Willowson *et al* 2008, Shcherbinin *et al* 2008) with similar results recently reported in patients where bladder activity was quantified (Zeintl *et al* 2010).

There is also increasing interest in the simultaneous use of dual radionuclides in a range of applications including heart (Ben-Haim *et al* 2010) and in brain (El Fakhri *et al* 2001). Here the correction of down-scatter has proved essential in order to separate the two radionuclides.

9.2. What are the barriers to implementation?

So why has the clinical implementation of scatter correction been so limited? There exists literature that states that the effect of scatter correction on image quality has had relatively little impact on clinical diagnosis (e.g. Bonnin *et al* 1994), with other factors having greater importance. It is true that attenuation correction and resolution modelling have more significant clinical impact, but optimal reconstruction quality and quantitative accuracy are to be expected only when the system model is complete, including accounting for scatter (see figure 6). There tends in the past to have been a practice of applying scatter correction without performing attenuation correction, which is not advisable; in contrast, when attenuation correction is performed, one should preferably also correct for scatter (Hutton 1997). Despite a growing literature that supports the use of scatter correction there is still reluctance to adopt scatter correction in routine clinical practice, even though recently some vendors have offered scatter correction methods as an option in their processing software. So far, application has largely been limited to specific centres with interest in quantitative studies. Despite strong evidence, the acceptance of need for routine attenuation correction, let alone scatter correction, has been slow. The most promising approaches to scatter correction tend to be based on quite sophisticated software that incorporates scatter modelling (sometimes based on MC modelling) directly in the reconstruction, and these have been demonstrated to be fast enough for clinical application. Unfortunately commercial suppliers have been slow to

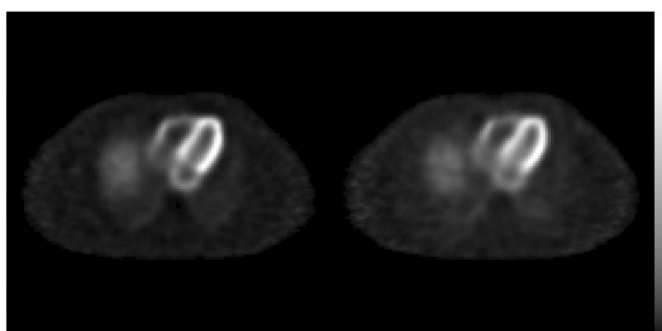


Figure 6. Reconstructions using attenuation correction and resolution modelling for Monte Carlo simulated data of the thorax without scatter (left) and with scatter (right). Improved contrast is observed when no scatter is present (equivalent to perfect scatter correction) e.g. between myocardium and ventricular cavity and between lungs and background (data courtesy Kjell Erlandsson, UCL).

introduce these techniques as part of their standard options, probably due to uncertainty in choice of approach, concerns regarding practical speed, lack of concrete validation data and lack of high priority expressed by the general clinical community. Only one of the three main suppliers of SPECT systems offers a scatter model (ESSE) to be used in conjunction with measured transmission data. The other two suppliers only offer TEW, one still falling short of the recommended implementation where the measurement can be directly included during reconstruction. Providers of workstations that include reconstruction software have various scatter correction solutions e.g. Nuclear Diagnostics recently introduced an option to purchase MC-based scatter estimation. Availability of scatter correction options for multi-radionuclide and multi-energy radionuclide studies also lags development, which is unfortunate given the potential benefits in these applications.

An alternative is open-source software, but this needs to be fast, reliable, easy to use, well documented and supported before this will satisfy even the research community, let alone the medical community. To a large extent, there is agreement in the physics community that scatter correction is essential for quantitative SPECT imaging, with the added advantage of improving signal-to-noise ratio, although there has been lack of consensus as to the optimal practical approach. Comparative studies tend in general to be undertaken by groups who compare their own developments with alternatives, with some doubt as to the optimization across all methods tested and few comparisons are totally comprehensive (e.g. Moore *et al* 2001). Interpretation of results can be difficult in the presence of various factors that can affect quantification (motion, partial volume effects) so at times isolation of concrete results regarding the impact of scatter correction is difficult. There is a definite need for standard datasets representing a range of applications to be made available across the medical community to facilitate cross-comparison of algorithms. Similar exercises have proven to be very effective in demonstrating optimal choice of registration algorithms (West *et al* 1997). There are moves in this direction from some quarters with Monte Carlo based libraries beginning to appear specifically for PET (Reilhac *et al* 2006, Castiglioni *et al* 2005) and recent work to establish cross-site comparability either for establishing common normal ranges (Dickson *et al* 2010) or demonstrating site compliance with standards for multi-centre clinical trials (Armato *et al* 2008, Meyer *et al* 2009, Frank 2008). Consensus on scatter correction is an important consideration of this work which deserves further attention.

10. Concluding discussion

Scatter correction is a topic that has been extensively studied over an extended period; this itself demonstrates that scatter problems in general are not trivial to solve. In clinical practice the tendency has been to adopt relatively easily implemented approaches such as TEW which are neither very accurate nor very robust to noise; consequently, clinical opinion as to the value of scatter correction has been somewhat tainted. It is only recently that more robust and accurate scatter correction techniques have been developed that, with presently available computational speed, can be implemented in a practical timescale; this is coupled with the relatively recent availability of SPECT/CT systems that provide a practical solution to attenuation correction. Provided turnkey solutions for scatter correction are available, the general practitioner may be more encouraged to perform studies that exploit truly quantitative reconstruction.

In PET, scatter correction is always performed, because quantitative reconstruction is systematic (at least relative quantification using SUV). In SPECT, the situation has been different because for a long time the accurate attenuation maps required to apply quantitative reconstruction methods were not present. There is however increasing demand for absolute activity estimation for dosimetry applications and continuing interest in deriving quantitative functional indices. Modern methods are well suited to respond to this demand: they are more generally applicable, they can improve noise properties and they are more accurate. Despite these attractive properties there may be difficulties to implement these methods on commercial systems.

Several suppliers provide options for scatter correction but these vary significantly across the vendors, ranging from simple TEW subtraction on projections to full Monte Carlo modelling. The correction has to be highly robust with respect to any prior or optional parameters and the correction should never introduce artefacts or strange values. Practitioners need to be confident that end results are truly comparable across systems. So ensuring robustness of the correction is a key point, which is not trivial to achieve given that a gamma camera performs many different types of scans. As a step towards standardization, it would be useful if recently developed approaches were optionally available on a wider basis. In time, perhaps we can anticipate that every correction may be optionally modelled during iterative reconstruction (as is already the case with PET). But until that time there is need for further demonstration of clinical use, to reach consensus within the user community as to the preferred method of correction, and solid product development which requires close collaboration of industry and academia.

Acknowledgments

BH is at UCL/UCLH which receives a component of research funding from the UK Department of Health NIHR Biomedical Research Centres funding scheme; he also acknowledges support from CRUK and EPSRC. FB is supported by the 3Binding PID Project, Dutch Economical Affairs.

References

- An S H, Seo H, Lee J H, Lee C S, Lee J S and Kim C H 2007 Effect of detector parameters on the image quality of Compton camera for ^{99m}Tc *Nucl. Instrum. Methods Phys. Res. A* **571** 251–4

- Armato S G, Meyer C R, McNitt-Gray M F, McLennan G, Reeves A P, Croft B Y and Clarke L P 2008 The reference image database to evaluate response to therapy in lung cancer (RIDER) project: a resource for the development of change-analysis software *Clin. Pharmacol. Ther.* **84** 448–56
- Assié K, Dieudonné A, Gardin I, Véra P and Buvat I 2010 A preliminary study of quantitative protocols in Indium 111 SPECT using computational simulations and phantoms *IEEE Trans. Nucl. Sci.* **57** 1096–104
- Axelsson B, Msaki R and Israelsson A 1984 Subtraction of Compton scattered photons in single-photon emission computerized tomography *J. Nucl. Med.* **25** 490–4
- Bailey D L, Hutton B F, Meikle S M, Fulton R R and Jackson C F 1989 Iterative scatter correction incorporating attenuation data *Eur. J. Nucl. Med.* **15** 452
- Bailey D L, Schembri G P, Harris B E, Bailey E A, Cooper R A and Roach P J 2008 Generation of planar images from lung ventilation/perfusion SPECT *Ann. Nucl. Med.* **22** 437–45
- Barnden L R, Dickson J and Hutton B F 2006 Detection and validation of the body edge in low count emission tomography images *Comput. Methods Programs Biomed.* **84** 153–61
- Beck J W, Jaszczak R J, Coleman R E, Starmer C F and Nolte L W 1982 Analysis of SPECT including scatter and attenuation using sophisticated Monte-Carlo modeling methods *IEEE Trans. Nucl. Sci.* **29** 506–11
- Beekman F J, de Jong H W A M and Slijpen E T P 1999 Efficient SPECT scatter calculation in non-uniform media using correlated Monte Carlo simulation *Phys. Med. Biol.* **44** N183–92
- Beekman F J, de Jong H W and van Geloven S 2002 Efficient fully 3-D iterative SPECT reconstruction with Monte Carlo-based scatter compensation *IEEE Trans. Med. Imaging* **21** 867–77
- Beekman F J, den Harder J M, Viergever M A and van Rijk P P 1997a SPECT scatter modeling in non-uniform attenuating objects *Phys. Med. Biol.* **42** 1133–42
- Beekman F J, Eijkman E G J, Viergever M A, Borm G F and Slijpen E T P 1993 Object shape dependent PSF model for SPECT imaging *IEEE Trans. Nucl. Sci.* **40** 31–9
- Beekman F J, Frey E C, Kamphuis C and Tsui B M W 1994 A new phantom for determination of the scatter response of a gamma camera *IEEE Trans. Nucl. Sci.* **41** 1481–8
- Beekman F J, Kamphuis C and Frey E C 1997b Scatter compensation methods in 3D iterative SPECT reconstruction: a simulation study *Phys. Med. Biol.* **42** 1619–32
- Beekman F J and Viergever M A 1995 Fast SPECT simulation including object shape dependent scatter *IEEE Trans. Med. Imaging* **14** 271–82
- Ben-Haim S *et al* 2010 Simultaneous dual-radionuclide myocardial perfusion imaging with a solid-state dedicated cardiac camera *Eur. J. Nucl. Med. Mol. Imaging* **37** 1710–21
- Bonnin F, Buvat I, Benali H and Di Paola R 1994 A comparative clinical study of scatter correction methods for scintigraphic images *Eur. J. Nucl. Med.* **21** 388–93
- Bowsher J E and Floyd C E 1991 Treatment of Compton scattering in maximum likelihood, expectation maximization reconstruction of SPECT images *J. Nucl. Med.* **32** 1285–91
- Bronnikov A V 2000 Reconstruction of attenuation map using discrete consistency conditions *IEEE Trans. Med. Imaging* **19** 451–62
- Bullich S, Cot A, Gallego J, Gunn R N, Suárez M, Pavía J, Ros D, Laruelle M and Catafau A M 2010 Impact of scatter correction on D2 receptor occupancy measurements using ¹²³I-IBZM SPECT: comparison to ¹¹C-Raclopride PET *Neuroimage* **50** 1511–8
- Buvat I, Benali H, Frouin F, Bazin J P and Di Paola R 1993 Target apex-seeking in factor analysis of medical image sequences *Phys. Med. Biol.* **38** 123–38
- Buvat I, Benali H, Todd-Pokropek A and Di Paola R 1994 Scatter correction in scintigraphy: the state of the art *Eur. J. Nucl. Med.* **21** 675–94
- Buvat I, Benali H, Todd-Pokropek A and Di Paola R 1995a A new correction method for gamma camera non-uniformity due to energy response variability *Phys. Med. Biol.* **40** 1357–74
- Buvat I, De Sousa M C, Di Paola M, Ricard M, Lumbroso J and Aubert B 1998 Impact of scatter correction in planar scintimammography: a phantom study *J. Nucl. Med.* **39** 1590–96
- Buvat I, Rodriguez-Villafuerte M, Todd-Pokropek A, Benali H and Di Paola R 1995b Comparative assessment of nine scatter correction methods based on spectral analysis using Monte Carlo simulations *J. Nucl. Med.* **36** 1476–88
- Cade S C, Bousse A, Arridge S, Evans M J and Hutton B F 2010 Estimating an attenuation map from measured scatter for 180° cardiac SPECT *J. Nucl. Med.* **51** 1357
- Castiglioni I, Buvat I, Rizzo G, Gilardi M C, Feuardent J and Fazio F 2005 A publicly accessible Monte Carlo database for validation purposes in emission tomography *Eur. J. Nucl. Med. Mol. Imaging* **32** 1234–9
- Chang L T 1978 A method for attenuation correction in radionuclide computed tomography *IEEE Trans. Nucl. Sci.* **25** 638–43
- Chen C L, Wang Y, Lee J J and Tsui B M 2009 Toward quantitative small animal pinhole SPECT: assessment of quantitation accuracy prior to image compensations *Mol. Imaging Biol.* **11** 195–203

- Cot A *et al* 2005 Absolute quantification in dopaminergic neurotransmission SPECT using a Monte Carlo-based scatter correction and fully 3-dimensional reconstruction *J. Nucl. Med.* **46** 1497–504
- Cot A *et al* 2006 Modeling of high energy contamination in SPECT imaging using Monte Carlo simulation *IEEE Trans. Nucl. Sci.* **53** 198–203
- Cot A *et al* 2004 Study of the point spread function (PSF) for ^{123}I SPECT imaging using Monte Carlo simulation *Phys. Med. Biol.* **49** 3125–36
- Crepaldi F and De Pierro A R 2007 Activity and attenuation reconstruction for positron emission tomography using emission data only via maximum likelihood and iterative data refinement *IEEE Trans. Nucl. Sci.* **54** 100–6
- Crespo C *et al* 2008 Quantification of dopaminergic neurotransmission SPECT studies with (123)I-labelled radioligands. A comparison between different imaging systems and data acquisition protocols using Monte Carlo simulation *Eur. J. Nucl. Med. Mol. Imaging* **35** 1334–42
- De Beenhouwer J, Staelens S, Vandenberghe S and Lemahieu I 2008 Acceleration of GATE SPECT simulations *Med. Phys.* **35** 1476–85
- De Jong H W A M and Beekman F J 2001a Rapid SPECT simulation of down scatter in non-uniform media *Phys. Med. Biol.* **46** 621–35
- De Jong H W A M, Beekman F J and Slijpen E T P 2001b Acceleration of Monte Carlo SPECT simulation using convolution-based forced detection *IEEE Trans. Nucl. Sci.* **48** 58–64
- De Jong H W A M, Beekman F J, Viergever M A and van Rijk P P 2002a Simultaneous (99m)Tc/(201)Tl dual-isotope SPET with Monte Carlo-based down-scatter correction *Eur. J. Nucl. Med. Mol. Imaging* **29** 1063–71
- De Jong H W A M, Wang W T, Frey E C, Viergever M A and Beekman F J 2002b Efficient simulation of SPECT down-scatter including photon interactions with crystal and lead *Med. Phys.* **29** 550–60
- De Vries D J, King M A, Soares E J, Tsui B M W and Metz C E 1999 Effects of scatter subtraction on detection and quantitation in hepatic SPECT *J. Nucl. Med.* **40** 1011–23
- De Wit T C, Xiao J and Beekman F J 2005 Monte Carlo based statistical SPECT reconstruction: influence of number of photon tracks *IEEE Trans. Nucl. Sci.* **52** 1365–9
- Descourt P, Carlier T, Du Y, Song X, Buvat I, Frey E C, Bardies M, Tsui B M and Visvikis D 2010 Implementation of angular response function modeling in SPECT simulations with GATE *Phys. Med. Biol.* **55** N253–66
- De Vito R P and Hamill J J 1991 Determination of weighting functions for energy weighted acquisition *J. Nucl. Med.* **32** 343–9
- De Vito R P, Hamill J J, Treffert J D and Stoub E W 1989 Energy-weighted acquisition of scintigraphic images using spatial filters *J. Nucl. Med.* **30** 2029–35
- Dewaraja Y K, Ljungberg M and Fessler J A 2006 3D Monte Carlo-based scatter compensation in quantitative I-131SPECT reconstruction *IEEE Trans. Nucl. Sci.* **253** 181–8
- Dewaraja Y K, Ljungberg M and Koral K F 2000 Characterization of scatter and penetration using Monte Carlo simulation in ^{131}I imaging *J. Nucl. Med.* **41** 123–30
- Dewaraja Y K, Wilderman S J, Ljungberg M, Koral K F, Zasadny K and Kaminiski M S 2005 Accurate dosimetry in I-131 radionuclide therapy using patient-specific, 3-dimensional methods for SPECT reconstruction and absorbed dose calculation *J. Nucl. Med.* **46** 840–9
- Dickson J C, Tossici-Bolt L, Sera T, Erlandsson K, Varrone A, Tatsch K and Hutton B F 2010 The impact of reconstruction method on the quantification of DaTSCAN images *Eur. J. Nucl. Med. Mol. Imaging* **37** 23–35
- Dobbeleir A A, Hambye A E and Franken P R 1999 Influence of high-energy photons on the spectrum of iodine-123 with low- and medium-energy collimators: consequences for imaging with iodine-123 labelled compounds in clinical practice *Eur. J. Nucl. Med.* **26** 655–8
- Du Y and Frey E C 2009 Quantitative evaluation of simultaneous reconstruction with model-based crosstalk compensation for $^{99\text{m}}\text{Tc}/^{123}\text{I}$ dual-isotope simultaneous acquisition brain SPECT *Med. Phys.* **36** 2021–30
- Du Y, Tsui B M and Frey E C 2006 Model-based compensation for quantitative ^{123}I brain SPECT imaging *Phys. Med. Biol.* **51** 1269–82
- Du Y, Tsui B M and Frey E C 2007 Model-based crosstalk compensation for simultaneous $^{99\text{m}}\text{Tc}/^{123}\text{I}$ dual-isotope brain SPECT imaging *Med. Phys.* **34** 3530–43
- Eberl S 2000 Quantitative physiological parameter estimation from dynamic SPECT *PhD Thesis* University NSW, Sydney
- El Fakhri G, Buvat I, Benali H, Todd-Pokropek A and Di Paola R 2000a Relative impact of scatter, collimator response, attenuation, and finite spatial resolution corrections in cardiac SPECT *J. Nucl. Med.* **41** 1400–8
- El Fakhri G *et al* 2000b Scatter and cross-talk corrections in simultaneous Tc-99m/I-123 brain SPECT using constrained factor analysis and artificial neural networks *IEEE Trans. Nucl. Sci.* **47** 1573–80
- El Fakhri G, Moore S C and Kijewski M F 2002 Optimization of Ga-67 imaging for detection and estimation tasks: dependence of imaging performance on spectral acquisition parameters *Med. Phys.* **29** 1859–66

- El Fakhri G, Moore S C, Maksud P, Aurengo A and Kijewski M F 2001 Absolute activity quantitation in simultaneous $^{123}\text{I}/^{99\text{m}}\text{Tc}$ brain SPECT *J. Nucl. Med.* **42** 300–8
- Farncombe T H, Gifford H C, Narayanan M V, Pretorius P H, Frey E C and King M A 2004 Assessment of scatter compensation strategies for (67)Ga SPECT using numerical observers and human LROC studies *J. Nucl. Med.* **45** 802–12
- Floyd C E, Jaszczak R J and Coleman R E 1989 Inverse Monte Carlo: a unified reconstruction algorithm *IEEE Trans. Nucl. Sci.* **32** 779–85
- Floyd C E, Jaszczak R J, Greer K L and Coleman C E 1986 Inverse Monte Carlo as a unified reconstruction algorithm for ECT *J. Nucl. Med.* **27** 1577–85
- Floyd J L, Mann R B and Shaw A 1991 Changes in quantitative thallium-201 results associated with the use of energy-weighted acquisition *J. Nucl. Med.* **32** 805–7
- Frank R 2008 Quantitative imaging biomarkers alliance FDG-PET/CT working group report *Mol. Imaging Biol.* **10** 305
- Frey E C, Gilland K L and Tsui B M 2002 Application of task-based measures of image quality to optimization and evaluation of three-dimensional reconstruction-based compensation methods in myocardial perfusion SPECT *IEEE Trans. Med. Imaging* **21** 1040–50
- Frey E C, Ju Z W and Tsui B M W 1993 A fast projector-backprojector pair modeling the asymmetric, spatially varying scatter response function for scatter compensation in SPECT imaging *IEEE Trans. Nucl. Sci.* **40** 1192–7
- Frey E C and Tsui B M W 1993 A practical method for incorporating scatter in a projector-backprojector for accurate scatter compensation in SPECT *IEEE Trans. Nucl. Sci.* **40** 1107–16
- Frey E C and Tsui B M W 1996 A new method for modeling the spatially variant, object-dependent scatter response function in SPECT *IEEE Nucl. Sci. Symp. Med. Imaging Conf.* **2** 1082–6
- Gagnon D, Laperrière L, Pouliot N, Arseneault A, Grégoire J and Dupras G 1990 Implementation of holospectral imaging on gamma camera *J. Nucl. Med.* **31** 758–9
- Gilardi M C, Bettinardi V, Todd-Pokropek A, Milanese L and Fazio F 1988 Assessment and comparison of three scatter correction techniques in single photon emission computed tomography *J. Nucl. Med.* **29** 1971–9
- Goorden M C and Beekman F J 2010 High-resolution tomography of positron emitters with clustered pinholes *Phys. Med. Biol.* **55** 1265–77
- Gur Y S *et al* 2002 Comparison of scatter compensation strategies for myocardial perfusion imaging using Tc-99m labeled sestamibi *IEEE Trans. Nucl. Sci.* **49** 2309–14
- Halama J R, Henkin R E and Friend L E 1988 Gamma camera radionuclide images: improved contrast with energy-weighted acquisition *Radiology* **169** 533–8
- Hamill J J and DeVito R P 1989 Scatter reduction with energy-weighted acquisition *IEEE Trans. Nucl. Sci.* **36** 1334–9
- Hapdey S, Soret M and Buvat I 2006 Quantification in simultaneous $^{99\text{m}}\text{Tc}/^{123}\text{I}$ brain SPECT using generalized spectral factor analysis: a Monte Carlo study *Phys. Med. Biol.* **51** 6157–71
- Harkness L J *et al* 2009a Optimisation of a dual head semiconductor Compton camera using Geant4 *Nucl. Instrum. Methods Phys. Res. A* **604** 351–4
- Harkness L *et al* 2009b Development of the ProSPECTus semiconductor Compton camera for medical imaging *IEEE Nucl. Sci. Symp. Conf.* pp 2452–5
- Harris C C, Greer K L, Jaszczak R J, Floyd C E, Fearnow E C and Coleman R E 1984 Tc-99m attenuation coefficients in water-filled phantoms determined with gamma cameras *Med. Phys.* **11** 681–5
- Hashimoto J, Kubo A, Ogawa K, Amano T, Fukuuchi Y, Motomura N and Ichihara T 1997 Scatter and attenuation correction in technetium-99m brain SPECT *J. Nucl. Med.* **38** 157–62
- He B and Frey E C 2006 Comparison of conventional, model-based quantitative planar, and quantitative SPECT image processing methods for organ activity estimation using In-111 agents *Phys. Med. Biol.* **51** 3967–81
- Hutton B F 1997 Cardiac single-photon emission tomography: is attenuation correction enough? *Eur. J. Nucl. Med.* **24** 713–5
- Hutton B F and Baccarne V 1998 Efficient scatter modeling for incorporation in maximum likelihood reconstruction *Eur. J. Nucl. Med.* **25** 1658–65
- Hutton B F, Osiecki A and Meikle S R 1996 Transmission-based scatter correction of 180 degree myocardial single photon emission tomographic studies *Eur. J. Nucl. Med.* **23** 1300–8
- Hwang A B *et al* 2008 Assessment of the sources of error affecting the quantitative accuracy of SPECT imaging in small animals *Phys. Med. Biol.* **53** 2233–52
- Ichihara T, Ogawa K, Motomura N, Kubo A and Hashimoto S 1993 Compton scatter compensation using the Triple-Energy Window method for single- and dual-isotope SPECT *J. Nucl. Med.* **34** 2216–21
- Iida H, Eberl S, Kim K M, Tamura Y, Ono Y, Nakazawa M, Sohlberg A, Zeniya T, Hayashi T and Watabe H 2008 Absolute quantitation of myocardial blood flow with (201)Tl and dynamic SPECT in canine: optimisation and validation of kinetic modeling *Eur. J. Nucl. Med. Mol. Imaging* **35** 896–905

- Iida H *et al* 1998 Effects of scatter and attenuation correction on quantitative assessment of regional cerebral blood flow with SPECT *J. Nucl. Med.* **39** 181–9
- Jaszczak R J, Coleman R E and Whitehead F R 1981 Physical factors affecting quantitative measurements using camera-based single photon-emission computed-tomography (SPECT) *IEEE Trans. Nucl. Sci.* **28** 69–80
- Jaszczak R J, Greer K L, Floyd C E, Harris C C and Coleman R E 1984 Improved SPECT quantification using compensation for scattered photons *J. Nucl. Med.* **25** 893–900
- Jaszczak R J, Hoffman D C and DeVito R P 1991 Variance propagation for SPECT with energy-weighted acquisition *IEEE Trans. Nucl. Sci.* **38** 739–47
- Kacperski K, Erlandsson K, Ben-Haim S, Van Gramberg D and Hutton B F 2011 Iterative deconvolution of simultaneous ^{99m}Tc and ^{201}Tl projection data measured on a CdZnTe based cardiac SPECT scanner *Phys. Med. Biol.* **56** 1397–414
- Kado H *et al* 2001 Brain perfusion SPECT study with ^{99m}Tc -bicisate: clinical pitfalls and improved diagnostic accuracy with a combination of linearization and scatter-attenuation correction *Ann. Nucl. Med.* **15** 123–9
- Kadrmas D J, Frey E C, Karimi S S and Tsui B M 1998 Fast implementations of reconstruction-based scatter compensation in fully 3D SPECT image reconstruction *Phys. Med. Biol.* **43** 857–73
- Kamphuis C, Beekman F J, van Rijk P P and Viergever M A 1998 Dual matrix ordered subsets reconstruction for accelerated 3D scatter compensation in single-photon emission tomography *Eur. J. Nucl. Med.* **25** 8–18
- Khosravi H R *et al* 2007 Planar and SPECT Monte Carlo acceleration using a variance reduction technique in I-131 imaging *Iran. J. Radiat. Res.* **4** 175–82
- Kim K M, Watabe H, Shidahara M, Ishida M and Iida H 2001a SPECT collimator dependency of scatter and validation of transmission dependent scatter compensation methodologies *IEEE Trans. Nucl. Sci.* **48** 689–96
- Kim K M *et al* 2001b Effect of scatter correction on quantitative estimation in receptor ligand study with SPECT *J. Nucl. Med.* **42** 184P
- King M A, Coleman M, Penney B C and Glick S J 1991 Activity quantitation in SPECT: a study of prereconstruction Metz filtering and use of the scatter degradation factor *Med. Phys.* **18** 184–9
- King M A, deVries D J, Pan T S, Pretorius P H and Case J A 1997 An investigation of the filtering of TEW scatter estimates used to compensate for scatter with ordered subset reconstructions *IEEE Trans. Nucl. Sci.* **44** 1140–45
- King M A, Hademenos G J and Glick S J 1992 A dual-photo-peak window method for scatter correction *J. Nucl. Med.* **33** 605–12
- Knesaurek K and Machac J 2000 Comparison of correction techniques for simultaneous $^{201}\text{Tl}/^{99m}\text{Tc}$ myocardial perfusion SPECT imaging: a dog study *Phys. Med. Biol.* **45** N167–76
- Koral K F 1998 Monte Carlo in SPECT scatter correction *Monte Carlo Calculations in Nuclear Medicine: Applications in Diagnostic Imaging* ed M Ljungberg, S-E Strand and M A King (Bristol: Institute of Physics Publishing) pp 165–81
- Koral K F, Wang X, Rogers W L, Clinthorne N H and Wang X 1988 SPECT Compton scattering correction by analysis of energy spectra *J. Nucl. Med.* **29** 195–202
- Kurosawa S *et al* 2010 Development of an 8×8 array of LaBr₃(Ce) scintillator pixels for a gaseous Compton gamma-ray camera *Nucl. Instrum. Methods Phys. Res. A* **623** 249–51
- Lange K and Carson R 1984 EM reconstruction algorithms for emission and transmission tomography *J. Comput. Assist. Tomogr.* **8** 306–16
- Laurette I, Zeng G L, Welch A, Christian P E and Gullberg G T 2000 A three-dimensional ray-driven attenuation, scatter and geometric response correction technique for SPECT in inhomogeneous media *Phys. Med. Biol.* **45** 3459–80
- Lazaro D, El Bitar Z, Breton V, Hill D and Buvat I 2005 Fully 3D Monte Carlo reconstruction in SPECT: a feasibility study *Phys. Med. Biol.* **50** 3739–54
- Liu S Y *et al* 2008 Convolution-based forced detection Monte Carlo simulation incorporating septal penetration modeling *IEEE Trans. Nucl. Sci.* **55** 967–74
- Ljungberg M, King M A, Hademenos G J and Strand S E 1994 Comparison of four scatter correction methods using Monte Carlo simulated source distributions *J. Nucl. Med.* **35** 143–51
- Ljungberg M and Strand S E 1989 A Monte Carlo program for the simulation of scintillation camera characteristics *Comput. Methods Programs Biomed.* **29** 257–72
- Ljungberg M and Strand S E 1990 Scatter and attenuation correction in SPECT using density maps and Monte Carlo simulated scatter functions *J. Nucl. Med.* **31** 1560–7
- Maor D, Berlad G, Chrem Y, Voil A and Todd-Pokropek A 1991 Klein–Nishina based energy factors for Compton free imaging (CFI) *J. Nucl. Med.* **32** 1000
- Mas J, Hannequin P, Ben Younes R, Bellaton B and Bidet R 1990 Scatter correction in planar imaging and SPECT by constrained factor analysis of dynamic structures (FADS) *Phys. Med. Biol.* **35** 1451–65
- Matsudaira M, Nakajima K, Tonami N and Hisada K 1997 Dual isotope SPECT with ^{99m}Tc and ^{123}I using four-energy-window (FEW) method *Kaku Igaku* **34** 1013–20

- Meikle S R, Hutton B F and Bailey D L 1994 A transmission-dependent method for scatter correction in SPECT *J. Nucl. Med.* **35** 360–7
- Meyer C R *et al* 2009 Quantitative imaging to assess tumor response to therapy: common themes of measurement, truth data, and error sources *Transl. Oncol.* **2** 198–210
- Monville M and O'Connor M K 1997 Optimization of acquisition and processing parameters in the Compton-free imaging (CFI) scatter correction technique *J. Nucl. Med.* **38** 67P
- Moore S C, English R J, Syravanh C, Tow D E, Zimmerman R E, Chan K H and Kijewski M F 1995 Simultaneous Tc-99m/Tl-201 imaging using energy-based estimation of the spatial distributions of contaminant photons *IEEE Trans. Nucl. Sci.* **42** 1189–95
- Moore S C, Kijewski M F, Muller S P, Rybicki F and Zimmerman R E 2001 Evaluation of scatter compensation methods by their effects on parameter estimation from SPECT projections *Med. Phys.* **28** 278–87
- Msaki P, Axelsson B, Dahl C M and Larsson S A 1987 Generalized scatter correction method in SPECT using point scatter distribution functions *J. Nucl. Med.* **28** 1861–9
- Narayanan M V *et al* 2003 Evaluation of scatter compensation strategies and their impact on human detection performance Tc-99m myocardial perfusion imaging *IEEE Trans. Nucl. Sci.* **50** 1522–7
- Narita Y, Eberl S, Iida H, Hutton B F, Braun M, Nakamura T and Bautovich G 1996 Monte Carlo and experimental evaluation of accuracy and noise properties of two scatter correction methods for SPECT *Phys. Med. Biol.* **41** 2481–96
- Nunez M, Prakash V, Vila R, Mut F, Alonso O and Hutton B F 2009 Attenuation correction for lung SPECT: evidence of need and validation of an attenuation map derived from emission data *Eur. J. Nucl. Med. Mol. Imaging* **36** 1076–89
- Nunez M, Vila R, Alonso O, Beretta M and Mut F 2002 Scatter correction in scintimammography with ^{99m}Tc MIBI: preliminary results using phantom and clinical studies *World J. Nucl. Med.* **1** 55–60
- Nuyts J, Dupont P, Stroobants S, Beninck R, Mortelmans L and Suetens P 1999 Simultaneous maximum *a posteriori* reconstruction of attenuation and activity distributions from emission sinograms *IEEE Trans. Med. Imaging* **18** 393–403
- Ogawa K, Harata Y, Ichihara T, Kubo A and Hashimoto S 1991 A practical method for position-dependent Compton-scatter correction in single-photon emission CT *IEEE Trans. Med. Imaging* **10** 408–12
- Ouyang J, El Fakhri G and Moore S C 2007 Fast Monte Carlo based joint iterative reconstruction for simultaneous ^{99m}Tc/¹²³I SPECT imaging *Med. Phys.* **34** 3263–72
- Ouyang J, Zhu X, Trott C M and El Fakhri G 2009 Quantitative simultaneous ^{99m}Tc/¹²³I cardiac SPECT using MC-JOSEM *Med. Phys.* **36** 602–11
- Pan T, King M, Luo D, Dahlberg S and Villegas B 1997 Estimation of attenuation maps from scatter and photo-peak window single photon-emission computed tomographic images of technetium 99m-labeled sestamibi *J. Nucl. Cardiol.* **4** 42–51
- Pretorius P H, van Rensburg A J, van Aswegen A, Ltitler M G, Serfontein D E and Herbst C R 1993 The channel ratio method of scatter correction for radionuclide image quantitation *J. Nucl. Med.* **34** 330–5
- Reilhac A, Evans A C, Gimenez G and Costes N 2006 Creation and application of a simulated database of dynamic [18f]MPPF PET acquisitions incorporating inter-individual anatomical and biological variability *IEEE Trans. Med. Imaging* **25** 1431–9
- Riauka T A and Gortel Z W 1994 Photon propagation and detection in single-photon emission computed tomography—an analytical approach *Med. Phys.* **21** 1311–21
- Riauka T A, Hooper H R and Gortel Z W 1996 Experimental and numerical investigation of the 3D SPECT photon detection kernel for non-uniform attenuating media *Phys. Med. Biol.* **41** 1167–89
- Rosenthal M S, Cullom J, Hawkins W, Moore S C, Tsui B M and Yester M 1995 Quantitative SPECT imaging: a review and recommendations by the Focus Committee of the Society of Nuclear Medicine Computer and Instrumentation Council *J. Nucl. Med.* **36** 1489–513
- Segars W P, Lalush D S and Tsui B M W 1999 A realistic spline-based dynamic heart phantom *IEEE Trans. Nucl. Sci.* **46** 503–6
- Sgourous G, Frey E, Wahl R, He B, Prideaux A and Hobbs R 2008 Three-dimensional imaging-based radiobiological dosimetry *Semin. Nucl. Med.* **38** 321–34
- Shcherbinin S, Celler A, Belhocine T, Vanderwerf R and Driedger A 2008 Accuracy of quantitative reconstructions in SPECT/CT imaging *Phys. Med. Biol.* **53** 4595–604
- Shepp L A and Vardi Y 1982 Maximum likelihood reconstruction in positron emission tomography *IEEE Trans. Med. Imaging* **1** 113–22
- Shidahara M, Watabe H, Kim K M, Kato T, Kawatsu S, Kato R, Yoshimura K, Iida H and Ito K 2005 Development of a practical image-based scatter correction method for brain perfusion SPECT: comparison with the TEW method *Eur. J. Nucl. Med. Mol. Imaging.* **32** 1193–8

- Shidahara M *et al* 2002 Impact of attenuation and scatter correction on SPECT for quantification of cerebral blood flow using ^{99m}Tc ethyl cysteinate dimer *IEEE Trans. Nucl. Sci.* **49** 5–10
- Shinohara H *et al* 2000 Quantitative evaluation for scatter and attenuation correction in ^{99m}Tc SPECT—multicenter cooperation phantom study *Kaku Igaku* **37** 143–62
- Singh M and Doria D 1983 An electronically collimated gamma camera for single photon emission computed tomography *Med. Phys.* **10** 421–7
- Sitek A, Moore S C and Kijewski M F 2007 Correction for photon attenuation without transmission measurements using Compton scatter information in SPECT *IEEE Nucl. Symp. Sci. Conf. Record* pp 4210–2
- Sohlberg A, Watabe H and Iida H 2008a Three-dimensional SPECT reconstruction with transmission-dependent scattercorrection *Ann. Nucl. Med.* **22** 549–56
- Sohlberg A, Watabe H and Iida H 2008b Acceleration of Monte Carlo based scatter compensation for cardiac SPECT *Phys. Med. Biol.* **53** N277–85
- Song X, Segars W P, Du Y, Tsui B M W and Frey E C 2005 Fast modeling of the collimator–detector response in Monte Carlo simulation of SPECT imaging using the angular response function *Phys. Med. Biol.* **50** 1791–804
- Soret M, Koulibaly P M, Darcourt J, Hapdey S and Buvat I 2003 Quantitative accuracy of dopaminergic neurotransmission imaging with ^{123}I SPECT *J. Nucl. Med.* **44** 1184–93
- Staelens S G, de Wit T C, Lemahieu I A and Beekman F J 2008 Degradation of myocardial perfusion SPECT images caused by contaminants in thallos (201Tl) chloride *Eur. J. Nucl. Med. Mol. Imaging* **35** 922–32
- Staelens S, de Wit T and Beekman F 2007 Fast hybrid SPECT simulation including efficient septal penetration modeling (SP-PSF) *Phys. Med. Biol.* **52** 3027–43
- Staelens S, Vunckx K, de Beenhouwer J, Beekman F, D'Asseler Y, Nuyts J and Lemahieu I 2006 GATE simulations for optimization of pinhole imaging *Nucl. Instrum. Methods Phys. Res. A* **569** 359–63
- van der Have F and Beekman F J 2004 Photon penetration and scatter in micro-pinholes imaging: a Monte Carlo imaging *Phys. Med. Biol.* **49** 1369–86
- van der Have F and Beekman F J 2006 Characterization of photon penetration and scatter in golden keel-edge micro-pinholes *IEEE Trans. Nucl. Sci.* **53** 2635–45
- van der Have F, Vastenhouw B, Ramaker R M, Branderhorst W, Krah J O, Ji C, Staelens S G and Beekman F J 2009 U-SPECT-II: an ultra-high-resolution device for molecular small-animal imaging *J. Nucl. Med.* **50** 599–605
- Vanhove C, Defrise M, Bossuyt A and Lahoutte T 2009 Improved quantification in single-pinhole and multiple-pinhole SPECT using micro-CT information *Eur. J. Nucl. Med. Mol. Imaging* **36** 1049–63
- Vija H, Kaplan M S and Haynor D R 1999 Simultaneous estimation of SPECT activity and attenuation distributions from measured phantom data using a differential attenuation method *IEEE NSS MIC Conf. Records* vol 2 pp 884–8
- Welch A, Gullberg G T, Christian P E, Datz F L and Morgan H T 1995 A transmission-map-based scatter correction technique for SPECT in inhomogeneous media *Med. Phys.* **22** 1627–35
- Wells R G, Celler A and Harrop R 1998 Analytical calculation of photon distributions in SPECT projections *IEEE Trans. Nucl. Sci.* **45** 3202–14
- West J M *et al* 1997 Comparison and evaluation of retrospective intermodality brain image registration techniques *J. Comput. Assist. Tomogr.* **21** 554–66
- Willowson K, Bailey D L and Baldock C 2008 Quantitative SPECT reconstruction using CT-derived corrections *Phys. Med. Biol.* **53** 3099–112
- Wu C, van der Have F, Vastenhouw B, Dierckx R A, Paans A M and Beekman F J 2010 Absolute quantitative total-body small-animal SPECT with focusing pinholes *Eur. J. Nucl. Med. Mol. Imaging* **37** 2127–35
- Xiao J, de Wit T C, Staelens S G and Beekman F J 2006 Evaluation of 3D Monte Carlo-based scatter correction for ^{99m}Tc cardiac perfusion SPECT *J. Nucl. Med.* **47** 1662–9
- Xiao J, de Wit T C, Zbijewski W, Staelens S G and Beekman F 2007 Evaluation of 3D Monte Carlo-based scatter correction for ^{201}Tl cardiac perfusion SPECT *J. Nucl. Med.* **48** 637–44
- Xiao J, Verzijlbergen F, Viergever M A and Beekman F J 2000 Small field-of-view dedicated cardiac SPECT systems: impact of projection truncation *Eur. J. Nucl. Med. Mol. Imaging* **37** 528–36
- Zaidi H 1996 Quantitative SPECT: recent developments in detector response, attenuation and scatter correction techniques *Physica Medica* **12** 1011–117
- Zaidi H and Hasegawa B 2003 Determination of the attenuation map in emission tomography *J. Nucl. Med.* **44** 291–315
- Zaidi H and Koral K F 2004a Scatter modeling and compensation in emission tomography *Eur. J. Nucl. Med. Mol. Imaging* **31** 761–82
- Zaidi H and Koral K F 2004b Scatter correction strategies in emission tomography *Quantitative Analysis in Nuclear Medicine Imaging* ed H Zaidi (New York: Kluwer/Plenum)

-
- Zaidi H and Montandon M L 2002 Which attenuation coefficient to use in combined attenuation and scatter corrections for quantitative brain SPECT? *Eur. J. Nucl. Med.* **29** 967–9
- Zeintl J, Vija A H, Yahil A, Hornegger J and Kuwert T 2010 Quantitative accuracy of clinical ^{99m}Tc SPECT/CT using ordered-subset expectation maximization with 3-dimensional resolution recovery, attenuation, and scatter correction *J. Nucl. Med.* **51** 921–8